Inorg. Chem. **2006**, *45*, 2581–2587

Synthesis, Structure, and Luminescent Properties of Microporous Lanthanide Metal–Organic Frameworks with Inorganic Rod-Shaped Building Units

Xiaodan Guo, Guangshan Zhu,* Fuxing Sun, Zhongyue Li, Xiaojun Zhao, Xiaotian Li, Hanchang Wang, and Shilun Qiu*

State Key Laboratory of Inorganic Synthesis & Preparative Chemistry, Jilin University, Changchun 130012, China

Received November 1, 2005

A series of microporous lanthanide metal–organic frameworks, $Tb_3(BDC)_{4.5}(DMF)_2(H_2O)_3 \cdot (DMF)(H_2O)$ (**1**) and $Ln_3(BDC)_{4.5}(DMF)_2(H_2O)_3 \cdot (DMF)(C_2H_5OH)_{0.5}(H_2O)_{0.5}$ [Ln = Dy (**2**), Ho (**3**), Er (**4**)], have been synthesized by the reaction of the lanthanide metal ion (Ln^{3+}) with 1,4-benzenedicarboxylic acid and triethylenetetramine in a mixed solution of *N*,*N*′-dimethylformamide (DMF), water, and C_2H_5OH. X-ray diffraction analyses reveal that they are extremely similar in structure and crystallized in triclinic space group $P\bar{1}$. An edge-sharing metallic dimer and 4 metallic monomers assemble with 18 carboxylate groups to form discrete inorganic rod-shaped building units [$Ln_6(CO_2)_{18}$], which link to each other through phenyl groups to lead to three-dimensional open frameworks with approximately 4×6 Å rhombic channels along the [0,–1,1] direction. A water sorption isotherm proves that guest molecules in the framework of complex **1** can be removed to create permanent microporosity and about four water molecules per formula unit can be adsorbed into the micropores. These complexes exhibit blue fluorescence, and complex **1** shows a Tb^{3+} characteristic emission in the range of 450–650 nm.

Introduction

The construction of metal−organic frameworks (MOFs) through coordination of metal ions with multifunctional organic ligands is one of the current interests of a new class of porous materials.[1] These materials can be applied potentially in catalysis, gas storage, ion exchange, and molecular recognition as zeolites coming from open frameworks and exhibit amazing optical and magnetic properties arising from metal centers and ligands.[2] As functional metal centers, lanthanide metals have received intense attention for their special coordination properties to form isostructural complexes and fantastic physical and chemical characteristics. Many lanthanide MOFs have been synthesized, and most of them exhibit extraordinary optical and magnetic properties.[3] In contrast with transition-metal complexes, covalence plays a minor role in metal−ligand bonds of lanthanide complexes, and the nature of the coordination modes is controlled by metal−ligand and interligand steric interactions and also by the counteranion.[4] The high coordination number and flexible coordination geometry of lanthanide metal ions make it difficult to control the preparation of lanthanide complexes, but they are helpful in the formation of unusual molecular architectures.[5] As is known, lanthanide ions have a high

* To whom correspondence should be addressed. E-mail: sqiu@mail.jlu.edu.cn (S.Q.), zhugs@mail.jlu.edu.cn (G.Z.). Fax: (+86) 431 5168331.

(1) (a) Seo, J. S.; Whang, D.; Lee, H.; Jun, S. I.; Oh, J.; Jeon, Y. J.; Kim, K. *Nature* **2000**, *404*, 982. (b) Chen, B.; Eddaoudi, M.; Hyde, S. T.; O'Keeffe, M.; Yaghi, O. M. *Science* **2001**, *291*, 1021. (c) Sato, O.; Iyoda, T.; Fujishima, A.; Hashimoto, K. *Science* **1996**, *271*, 49. (d) Kahn, O.; Martinez, C. *Science* **1998**, *279*, 44.

(2) (a) Fang, Q.; Zhu, G.; Xue, M.; Sun, J.; Wei, Y.; Qiu, S.; Xu, R. *Angew. Chem., Int. Ed.* **2005**, *44*, 2. (b) Lin, W.; Evans, O. R.; Xiong, R.; Wang, Z. *J. Am. Chem. Soc.* **1998**, *120*, 13272. (c) Sun, J.; Weng, L.; Zhou, Y.; Chen, J.; Chen, Z.; Liu, Z.; Zhao, D. *Angew. Chem., Int. Ed.* **2002**, *41*, 4471. (d) Tian, G.; Zhu, G.; Yang, X.; Fang, Q.; Xue, M.; Sun, J.; Wei, Y.; Qiu, S. *Chem. Commun.* **2005**, 1396. (e) Devic, T.; Serre, C.; Audebrand, N.; Marrot, J.; Férey, G. *J. Am. Chem. Soc.* **2005**, *127*, 12788.

(3) (a) Liu, W. S.; Jiao, T. Q.; Li, Y. Z.; Liu, Q. Z.; Tan, M. Y.; Wang, H.; Wang, L. F. *J. Am. Chem. Soc.* **2004**, *126*, 2280. (b) Ma, B. Q.; Zhang, D. S.; Gao, S.; Jin, T. Z.; Yan, C. H.; Xu, G. X. *Angew. Chem., Int. Ed.* **2002**, *39*, 3644. (c) Serre, C.; Stock, N.; Bein, T.; Férey, G. *Inorg. Chem.* **2004**, *43*, 3159. (d) Mancino, G.; Ferguson, A. J.; Beeby, A.; Long, N. J.; Jones, T. S. *J. Am. Chem. Soc.* **2005**, *127*, 524. (e) Reineke, T. M.; Eddaoudi, M.; Fehr, M.; Kelley, D.; Yaghi, O. M. *J. Am. Chem. Soc.* **1999**, *121*, 1651. (f) Guo, X.; Zhu, G.; Fang, Q.; Xue, M.; Tian, G.; Sun, J.; Li, X.; Qiu, S. *Inorg. Chem.* **2004**, *44*, 3850.

(4) (a) Deluzet, A.; Maudez, W.; Daiguebonne, C.; Guillou, O. *Cryst. Growth Des.* **2003**, *3*, 475. (b) Ghosh, S. K.; Bharadwaj, P. K. *Inorg. Chem.* **2005**, *44*, 3156.

10.1021/ic0518881 CCC: $33.50
Published on Web 02/24/2006

Table 1. Crystallographic Data for Complexes **1**−**4**

	1	**2**	**3**	**4**
empirical formula	$C_{45}H_{47}Tb_3O_{25}N_3$	$C_{46}H_{49}Dy_3O_{25}N_3$	$C_{46}H_{49}Ho_3O_{25}N_3$	$C_{46}H_{49}Er_3O_{25}N_3$
fw	1506.6	1531.4	1538.7	1545.7
cryst syst	triclinc	triclinc	triclinc	triclinc
space group	$P\bar{1}$	$P\bar{1}$	$P\bar{1}$	$P\bar{1}$
a (Å)	10.7622(9)	10.7383(16)	10.741(2)	10.7098(5)
b (Å)	11.3038(10)	11.2808(16)	11.284(3)	11.2449(5)
c (Å)	26.224(2)	26.138(4)	26.152(6)	26.0660(11)
α (deg)	85.086(2)	85.111(3)	84.970(4)	84.9980(10)
β (deg)	88.092(2)	88.148(2)	87.963(4)	88.1350(10)
γ (deg)	62.225(2)	62.415(2)	62.568(4)	62.6600(10)
V (Å^3)	2812.3(4)	2796.0(7)	2802.5(11)	2777.8(2)
Z	2	2	2	2
T (K)	298(2)	298(2)	298(2)	298(2)
λ (Å)	0.71073	0.71073	0.71073	0.71073
ρ_{calc} (g/cm^3)	1.779	1.819	1.823	1.848
μ (mm^{-1})	3.813	4.051	4.277	4.574
R^a [$I > 20\sigma(I)$]	0.0746	0.0488	0.0408	0.0355
$R_w{}^b$	0.1641	0.1112	0.0763	0.0834

[a] $R = \sum||F_o| - |F_c||/\sum|F_o|$. [b] $R_w = [\sum w(F_o^2 - F_c^2)/\sum w(F_o^2)^2]^{1/2}$.

Table 2. Selected Bond Lengths (Å) for Complexes **1**

Complex **1**[a]

Tb1−O1	2.370(10)	Tb2−O4	2.290(10)	Tb3−O6$^{\#4}$	2.285(11)
Tb1−O2$^{\#1}$	2.304(11)	Tb2−O5$^{\#4}$	2.337(11)	Tb3−O13	2.374(11)
Tb1−O3	2.306(11)	Tb2−O8	2.313(11)	Tb3−O15$^{\#5}$	2.276(11)
Tb1−O7	2.277(11)	Tb2−O12	2.347(11)	Tb3−O19	2.450(11)
Tb1−O9$^{\#2}$	2.366(10)	Tb2−O14$^{\#5}$	2.395(11)	Tb3−O20	2.491(10)
Tb1−O9$^{\#3}$	2.527(11)	Tb2−O16	2.460(13)	Tb3−O21	2.462(12)
Tb1−O10$^{\#3}$	2.454(11)	Tb2−O17	2.445(13)	Tb3−O22	2.491(11)
Tb1−O11	2.389(13)	Tb2−O18	2.487(12)	Tb3−O23	2.405(11)

[a] Symmetry transformations used to generate equivalent atoms: #1, $-x + 1, -y, -z + 2$; #2, $-x + 2, -y, -z + 2$; #3, $x - 1, y, z$; #4, $x, y + 1, z$; #5, $x + 1, y, z$.

Table 3. Selected Bond Angles (deg) for Complexes **1**

Complex **1**[a]

O7−Tb1−O2$^{\#1}$	71.7(4)	O14$^{\#5}$−Tb2−O17	141.3(4)
O7−Tb1−O3	81.9(4)	O4−Tb2−O16	72.4(4)
O2$^{\#1}$−Tb1−O3	138.7(4)	O8−Tb2−O16	73.3(4)
O7−Tb1−O9$^{\#2}$	114.6(4)	O5$^{\#4}$−Tb2−O16	139.6(4)
O2$^{\#1}$−Tb1−O9$^{\#2}$	71.9(4)	O12−Tb2−O16	135.3(4)
O3−Tb1−O9$^{\#2}$	149.2(4)	O14$^{\#5}$−Tb2−O16	72.3(4)
O7−Tb1−O1	149.7(4)	O17−Tb2−O16	129.6(4)
O2$^{\#1}$−Tb1−O1	138.0(4)	O4−Tb2−O18	85.2(4)
O3−Tb1−O1	76.2(4)	O8−Tb2−O18	142.1(4)
O9$^{\#2}$−Tb1−O1	78.7(4)	O5$^{\#4}$−Tb2−O18	120.8(4)
O7−Tb1−O11	79.1(4)	O12−Tb2−O18	67.1(4)
O2$^{\#1}$−Tb1−O11	122.7(4)	O14$^{\#5}$−Tb2−O18	76.9(4)
O3−Tb1−O11	79.8(4)	O17−Tb2−O18	136.5(4)
O9$^{\#2}$−Tb1−O11	77.5(4)	O16−Tb2−O18	70.7(4)
O1−Tb1−O11	77.5(4)	O15$^{\#5}$−Tb3−O6$^{\#4}$	81.1(4)
O7−Tb1−O10$^{\#3}$	98.9(4)	O15$^{\#5}$−Tb3−O13	118.8(4)
O2$^{\#1}$−Tb1−O10$^{\#3}$	79.4(4)	O6$^{\#4}$−Tb3−O13	80.3(4)
O3−Tb1−O10$^{\#3}$	75.0(4)	O15$^{\#5}$−Tb3−O23	150.4(4)
O9$^{\#2}$−Tb1−O10$^{\#3}$	124.7(4)	O6$^{\#4}$−Tb3−O23	84.3(4)
O1−Tb1−O10$^{\#3}$	94.1(4)	O13−Tb3−O23	83.5(4)
O11−Tb1−O10$^{\#3}$	154.7(4)	O15$^{\#5}$−Tb3−O19	79.0(4)
O7−Tb1−O9$^{\#3}$	138.2(4)	O6$^{\#4}$−Tb3−O19	134.9(4)
O2$^{\#1}$−Tb1−O9$^{\#3}$	72.8(4)	O13−Tb3−O19	74.8(4)
O3−Tb1−O9$^{\#3}$	113.7(4)	O23−Tb3−O19	128.3(3)
O9$^{\#2}$−Tb1−O9$^{\#3}$	73.6(4)	O15$^{\#5}$−Tb3−O21	82.8(4)
O1−Tb1−O9$^{\#3}$	70.5(4)	O6$^{\#4}$−Tb3−O21	129.9(4)
O11−Tb1−O9$^{\#3}$	140.1(4)	O13−Tb3−O21	147.3(4)
O10$^{\#3}$−Tb1−O9$^{\#3}$	52.9(3)	O23−Tb3−O21	87.2(4)
O4−Tb2−O8	94.7(4)	O19−Tb3−O21	86.8(4)
O4−Tb2−O5$^{\#4}$	141.7(4)	O15$^{\#5}$−Tb3−O20	126.9(4)
O8−Tb2−O5$^{\#4}$	81.2(4)	O6$^{\#4}$−Tb3−O20	148.4(4)
O4−Tb2−O12	89.9(4)	O13−Tb3−O20	73.3(4)
O8−Tb2−O12	150.7(5)	O23−Tb3−O20	75.9(4)
O5$^{\#4}$−Tb2−O12	77.4(4)	O19−Tb3−O20	53.2(4)
O4−Tb2−O14$^{\#5}$	144.0(4)	O21−Tb3−O20	74.0(4)
O8−Tb2−O14$^{\#5}$	81.5(4)	O15$^{\#5}$−Tb3−O22	80.4(4)
O5$^{\#4}$−Tb2−O14$^{\#5}$	73.4(4)	O6$^{\#4}$−Tb3−O22	79.0(4)
O12−Tb2−O14$^{\#5}$	110.8(4)	O13−Tb3−O22	149.0(4)
O4−Tb2−O17	70.3(4)	O23−Tb3−O22	71.7(4)
O8−Tb2−O17	77.3(4)	O19−Tb3−O22	135.5(4)
O5$^{\#4}$−Tb2−O17	71.7(4)	O21−Tb3−O22	51.6(4)
O12−Tb2−O17	77.1(4)	O20−Tb3−O22	116.4(4)

[a] Symmetry transformations used to generate equivalent atoms: #1, $-x + 1, -y, -z + 2$; #2, $-x + 2, -y, -z + 2$; #3, $x - 1, y, z$; #4, $x, y + 1, z$; #5, $x + 1, y, z$.

affinity for hard donor atoms and ligands containing oxygen or hybrid oxygen−nitrogen atoms, especially multicarboxylate ligands, which are usually employed in the architectures for lanthanide coordination polymers.[6]

It has proven to be an effective method for the design and synthesis of open and rigid frameworks through the assembly of metal−carboxylate clusters with organic linkers. 1,4-Benzenedicarboxylic acid (H_2BDC) seems to be a promising organic linker because two carboxyl groups with a 180° angle are able to establish bridges between several metal centers through various coordination modes and the presence of conjugated aromatic rings allows it to become a rigid linker. A large number of coordination polymers made up of transition metals and H_2BDC have been reported, and many of them show excellent adsorption and gas-storage properties.[7] Compared with transition metals, the analogous lanthanide complexes are still undeveloped, though some lanthanide coordination polymers constructed from discrete metal−carboxylate clusters or infinite rod-shaped building units have been reported.[3e,4a,8] We here report a series of three-dimensional open frameworks constructed from discrete rod-shaped $Ln_6(CO_2)_{18}$ inorganic secondary building units (SBUs) with BDC linkers, $Tb_3(BDC)_{4.5}(DMF)_2(H_2O)_3 \cdot (DMF)$-

(5) (a) Kiritsis, V.; Michaelides, A.; Skoulika, S.; Golhen, S.; Ouahab, L. *Inorg. Chem.* **1998**, *37*, 3407. (b) Long, D. L.; Blake, A. J.; Champness, N. R.; Schroder, M. *Chem. Commun.* **2000**, 1369. (c) Long, D. L.; Blake, A. J.; Champness, N. R.; Wilson, C.; Schroder, M. *J. Am. Chem. Soc.* **2001**, *123*, 3401. (d) Wang, Z.; Jin, C. M.; Shao, T.; Li, Y. Z.; Zhang, K. L.; Zhang, H. T.; You, X. Z. *Inorg. Chem. Commun.* **2002**, *5*, 642.

(6) (a) Serre, C.; Férey, G. *J. Mater. Chem.* **2002**, *12*, 3053. (b) Serpaggi, F.; Férey, G. *J. Mater. Chem.* **1998**, *8*, 2749. (c) Serpaggi, F.; Férey, G. *Inorg. Chem.* **1999**, *38*, 4741.

(H_2O) (**1**) and $Ln_3(BDC)_{4.5}(DMF)_2(H_2O)_3\cdot(DMF)(C_2H_5OH)_{0.5}(H_2O)_{0.5}$ [Ln = Dy (**2**), Ho (**3**), Er (**4**)]. The thermal stability, water sorption, and luminescent properties have been investigated.

Experimental Section

All chemicals purchased were of reagent grade or better and were used without further purification. Lanthanide nitrate salts were prepared by dissolving lanthanide oxides with 6 M HNO_3, while adding a bit of H_2O_2 for Tb_4O_7, and then evaporating at 100 °C until the crystal film formed. Fluorescence spectroscopy data were recorded on a LS55 luminescence spectrometer. The elemental analyses were carried out on a Perkin-Elmer 240C elemental analyzer. The infrared (IR) spectra were recorded (400−4000-cm^{-1} region) on a Nicolet Impact 410 FTIR spectrometer using KBr pellets. Thermogravimetric analyses (TGA) were performed under an oxygen atmosphere with a heating rate of 5 °C/min using a Perkin-Elmer TGA 7 thermogravimetric analyzer.

Synthesis of $Tb_3(BDC)_{4.5}(DMF)_2(H_2O)_3\cdot(DMF)(H_2O)$ (1). A mixture of $Tb(NO_3)_3\cdot nH_2O$ (40 mg, 0.10 mmol) and 1,4-H_2BDC (16 mg, 0.10 mmol) was dissolved in *N*,*N*′-dimethylformamide (DMF; 10 mL), H_2O (2 mL), and C_2H_5OH (2 mL) at room temperature. Two drops of triethylenetetramine was added to that mixture, and then a bit of 6 M HNO_3 was added until the mixture became clear. The mixture in a 50-mL beaker was left undisturbed at 55 °C for 7 days to give colorless crystals. Yield: 82% (based on terbium). Elem anal. Calcd for $C_{45}H_{47}TbO_{25}N_3$ (1506.6): C, 35.87; H, 3.14; N, 2.79. Found: C, 35.48; H, 3.28; N, 2.77.

Synthesis of $Dy_3(BDC)_{4.5}(DMF)_2(H_2O)_3\cdot(DMF)(C_2H_5OH)_{0.5}(H_2O)_{0.5}$ (2). The procedure was the same as that for **1** except that $Tb(NO_3)_2\cdot nH_2O$ was replaced by $Dy(NO_3)_3\cdot nH_2O$ (40 mg, 0.10 mmol). Yield: 77% (based on dysprosium). Elem anal. Calcd for $C_{46}H_{49}DyO_{25}N_3$ (1531.4): C, 36.08; H, 3.23; N, 2.74. Found: C, 35.98; H, 3.26; N, 2.76.

Synthesis of $Ho_3(BDC)_{4.5}(DMF)_2(H_2O)_3\cdot(DMF)(C_2H_5OH)_{0.5}(H_2O)_{0.5}$ (3). The procedure was the same as that for **1** except that $Tb(NO_3)_2\cdot nH_2O$ was replaced by $Ho(NO_3)_3\cdot nH_2O$ (40 mg, 0.10 mmol). Yield: 75% (based on holmium). Elem anal. Calcd for $C_{46}H_{49}HoO_{25}N_3$ (1538.7): C, 35.91; H, 3.21; N, 2.73. Found: C, 35.94; H, 3.20; N, 2.74.

Synthesis of $Er_3(BDC)_{4.5}(DMF)_2(H_2O)_3\cdot(DMF)(C_2H_5OH)_{0.5}(H_2O)_{0.5}$ (4). The procedure was the same as that for **1** except that $Tb(NO_3)_2\cdot nH_2O$ was replaced by $Er(NO_3)_3\cdot nH_2O$ (40 mg, 0.10 mmol). Yield: 70% (based on erbium). Elem anal. Calcd for $C_{46}H_{49}ErO_{25}N_3$ (1545.7): C, 35.75; H, 3.20; N, 2.72. Found: C, 35.84; H, 3.18; N, 2.70.

X-ray Crystallographic Study. The intensity data were collected on a Smart CCD diffractometer with graphite-monochromated Mo Kα (λ = 0.710 73 Å) radiation at room temperature in the $\omega-2\theta$ scan mode. An empirical absorption correction was applied to the data using the *SADABS* program.[9] The structures were solved by direct methods. All non-hydrogen atoms were refined anisotropically. Hydrogen atoms were fixed at calculated positions and refined by using a riding mode. All calculations were performed using the *SHELXTL* program.[10] The crystallographic data are summarized in Table 1, the selected bond lengths and bond angles of complex **1** are listed in Tables 2 and 3, and the selected bond lengths and bond angles of complexes **2**−**4** are listed in Tables S1 and S2 of the Supporting Information, respectively.

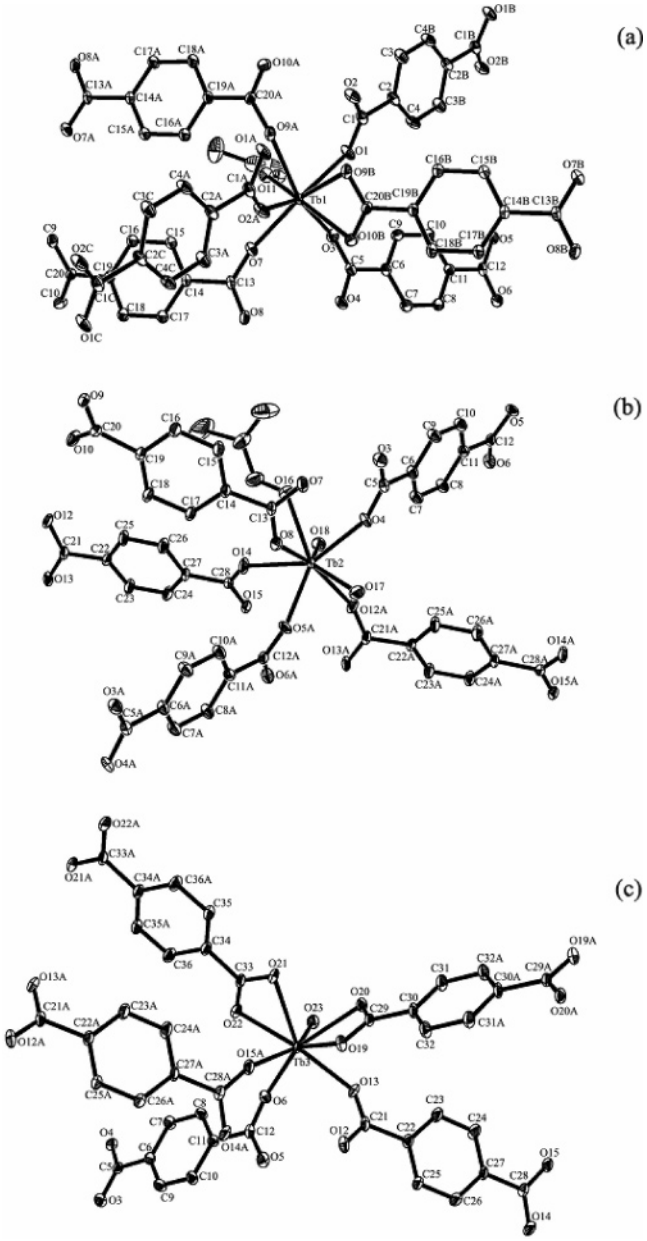

Figure 1. Coordination environments of (a) Tb1, (b) Tb2, and (c) Tb3 in complex **1** with non-hydrogen atoms represented by thermal ellipsoids drawn at the 30% probability level. Atoms labeled with additional A's and B's are symmetrically equivalent to those atoms without such designations.

Water Sorption Isotherm. Water sorption isotherm studies were performed by measuring the increase in weight at equilibrium as a function of the relative pressure. The weight of sample was measured by a Cahn 2000 electrobalance, and the adsorbate (H_2O) was added incrementally and manually.

(7) (a) Eddaoudi, M.; Kim, J.; Rosi, N.; Vodak, D.; Wachter, J.; O'Keeffe, M.; Yaghi, O. M. *Science* **2002**, *295*, 469. (b) Li, H.; Eddaoudi, M.; O'Keeffe, M.; Yaghi, O. M. *Nature* **1999**, *402*, 276. (c) Eddaoudi, M.; Li, H.; Yaghi, O. M. *J. Am. Chem. Soc.* **2000**, *122*, 1391. (d) Li, H.; Eddaoudi, M.; Groy, T. L.; Yaghi, O. M. *J. Am. Chem. Soc.* **1998**, *120*, 8571. (e) Férey, G.; Mellot-Draznieks, C.; Serre, C.; Millange, F.; Dutour, J.; Surblé, S.; Margiolaki, I. *Science* **2005**, *309*, 2040.

(8) (a) Pan, L.; Zheng, M.; Wu, Y.; Han, S.; Yang, R.; Huang, X.; Li, J. *Inorg. Chem.* **2001**, *40*, 828. (b) Serre, C.; Millange, F.; Marrot, J.; Férey, G. *Chem. Mater.* **2002**, *14*, 2409. (c) Reineke, T. M.; Eddaoudi, M.; Keeffe, M. O.; Yaghi, O. M. *Angew. Chem., Int. Ed.* **1999**, *38*, 2590.

(9) Sheldrick, G. M. *SADABS, Program for Empirical Absorption Correction for Area Detector Data*; University of Göttingen: Göttingen, Germany, 1996.

(10) Sheldrick, G. M. *SHELXS 97, Program for Crystal Structure Refinement*; University of Göttingen: Göttingen, Germany, 1997.

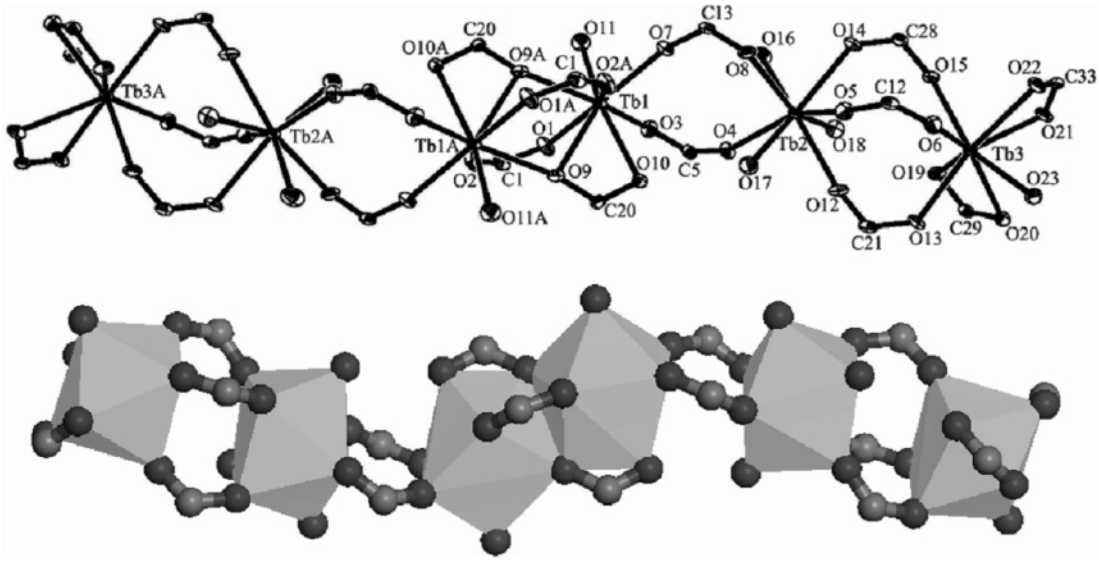

Figure 2. Three lanthanide metal center atoms (Tb1, Tb2, and Tb3) and their corresponding centrosymmetric atoms (Tb1A, Tb2A, and Tb3A) linked by 18 carboxyl groups of the BDC ligands to lead to a rod-shaped inorganic SBU [$Ln_6(CO_2)_{18}$].

Results and Discussion

Single-crystal X-ray diffraction (XRD), elemental analysis, and TGA analysis studies performed on the complexes **1**−**4** reveal that they are extremely similar in structure with slight differences in guest molecules. Here complex **1** is taken as an example to present and discuss the structure in detail.

Crystal Structure of Complex 1. An XRD study performed on complex **1** reveals that it is a three-dimensional framework, crystallizing in triclinic space group $P\bar{1}$. Each asymmetric unit [$(Tb_3(BDC)_{4.5}(DMF)_2(H_2O)_3\cdot(DMF)(H_2O)$] contains three eight-coordinated terbium ions, four and a half BDC ligands, two DMF molecules, three water molecules, one free DMF molecule, and one free water molecule. Three crystallographically different terbium atoms (Tb1, Tb2, and Tb3) are shown in Figure 1. Tb1 is coordinated with eight oxygen atoms from one chelating bidentate carboxyl group (O9 and O10), five dimonodentate carboxyl groups (O1, O2, O3, O7, and O9), and one terminal DMF molecule (O11) (Figure 1a). The eight oxygen atoms coordinated with Tb2 are from five dimonodentate carboxyl groups (O4, O5, O8, O12, and O14), one terminal DMF molecule (O16), and two terminal water molecules (O17 and O18) (Figure 1b). Tb3 is coordinated with four oxygen atoms from two different chelating bidentate carboxyl groups (O19, O20, O21, and O22), three oxygen atoms from three different dimonodentate carboxyl groups (O6, O13, and O15), and one terminal water molecule (O23) (Figure 1c). The carboxylic O−Tb, Tb−O_{wt}, and Tb−O_{DMF} bonds are in the ranges 2.290(6)−2.527(6), 2.405(11)−2.487(12), and 2.389(13)−2.460 (13) Å, respectively, all of which are comparable to those reported for other terbium−oxygen donor complexes.[3e,11] A lanthanide metal center atom (Tb1) and its corresponding centrosymmtric atom (Tb1A) link through four chelating/bridging

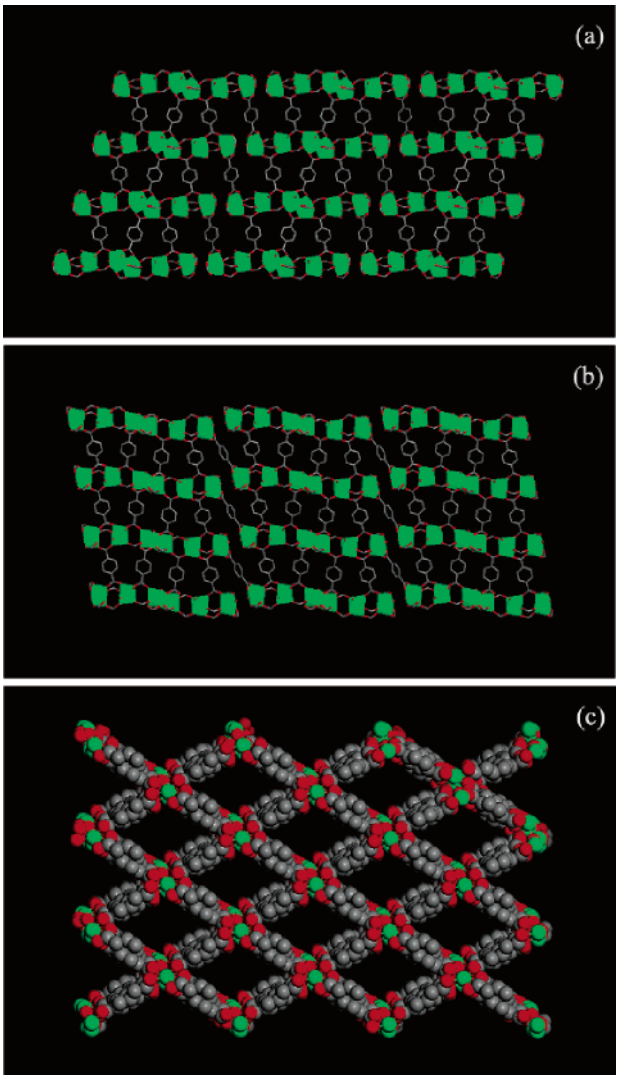

Figure 3. Rod-shaped inorganic SBUs [$Ln_6(CO_2)_{18}$] linked to each other by phenyl groups (a) on the (011) plane and (b) on the (100) plane. (c) One-dimensional channels viewed along the [011] direction (Tb, green; O, red; C, gray). Hydrogen atoms and parts of the DMF and water molecules are omitted for clarity.

(11) (a) Wan, Y.; Jin, L.; Wang, K.; Zhang, L.; Zheng, X.; Lu, S. *New J. Chem.* **2002**, *26*, 1590. (b) Liu, C. B.; Sun, C. Y.; Jin, L. P.; Lu, S. Z. *New J. Chem.* **2004**, *28*, 1019. (c) Sun, H. L.; Gao, S.; Ma, B. Q.; Chang, F.; Fu, W. F. *Microporous Mesoporous Mater.* **2004**, *73*, 89.

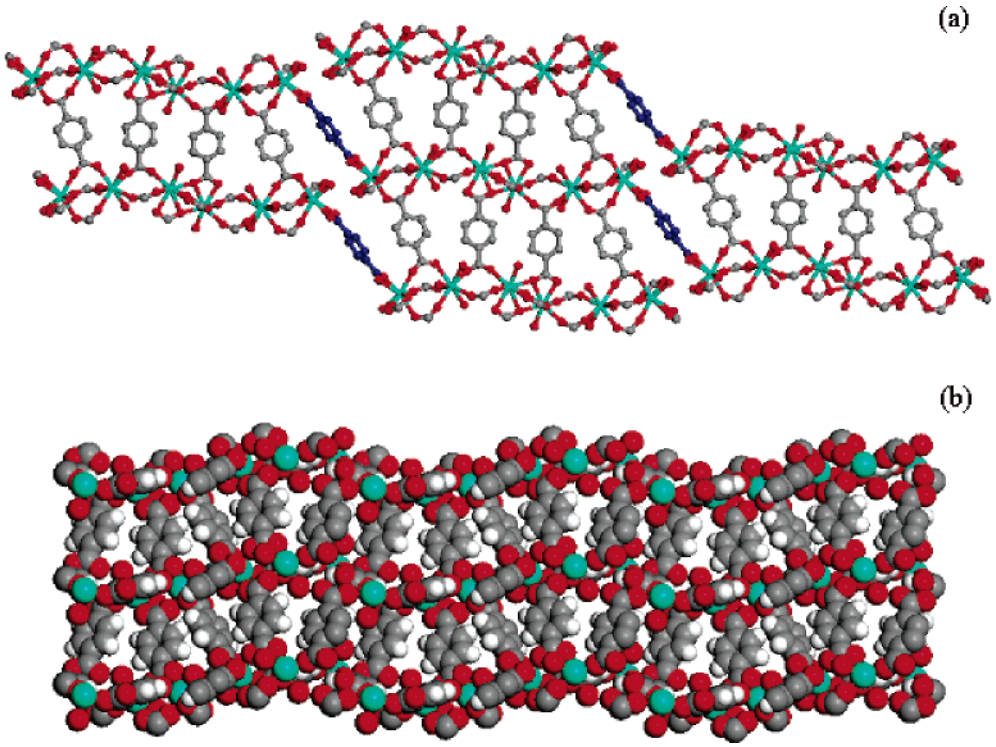

Figure 4. (a) BDC linkers (dark blue) connected with lanthanide ions (Tb3) at the end of the rod-shaped building units, adopting chelating bidentate coordination mode. (b) Impenetrable wall of the channels adjacent to ligand weak CH···π interactions of BDC, leading to the open framework without interpenetration.

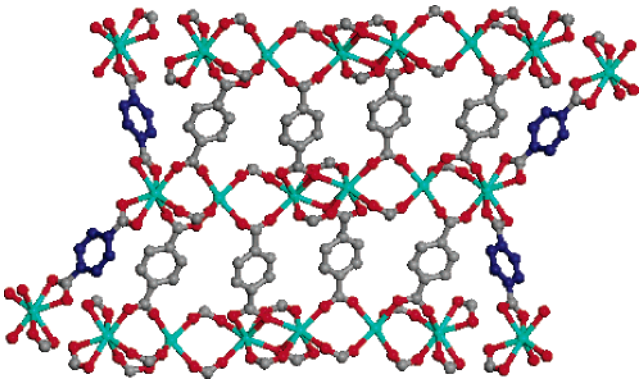

Figure 5. BDC ligands whose carboxylate groups (C, gray) adopted dimonodatate and chelating/bridging bidentate coordination modes are similar to the "linkers" of the infinite rod-shaped SBUs, and those (C, dark blue) adopted chelating bidentate mode like the "struts" to connect the hexameric units.

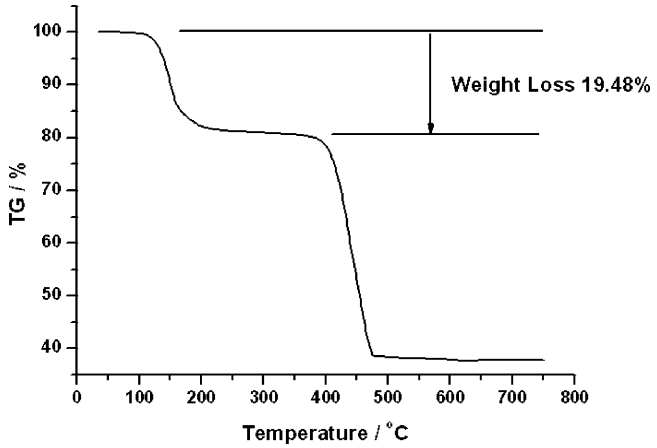

Figure 6. TGA curve of complex **1**.

bidentate carboxyl groups of BDC ligands to form an edge-sharing metallic dimer, as seen in Figure 2. The edge-sharing dimer (Tb1 and Tb1A) assembles with the four metallic monomers (Tb2, Tb2A, Tb3, and Tb3A) through carboxyl groups to lead to discrete inorganic rod-shaped building units [$Tb_3(CO_2)_{18}$]. These rod-shaped building units link to each other through phenyl groups of the BDC ligands on the (011) and (100) planes to form a three-dimensional framework with 4 × 6 Å rhombic channels along the [0,−1,1] direction (taking into account the van der Waals radii of the atoms; Figure 3).

Carefully examining the structure of complex **1**, we find that rod-shaped building units link to each other not to form infinite chains but to lead to pseudochains because the coordination modes of the BDC linkers are different at different positions. There are three coordination modes of the BDC linker: dimonodentate, chelating bidentate, and chelating/bridging bidentate (Chart S1 in the Supporting Information). The BDC linkers whose coordination modes are dimonodentate and chelating/bridging bidentate are used to connect two parallel rod-shaped building units. All of the BDC linkers adopting chelating bidentate coordination mode connect with lanthanide ions (Tb3) at the end of the rod-shaped building units, which prevents the rod-shaped building units from connecting to each other to form infinite inorganic chains as reported in other lanthanide MOFs (Figure 4a).[3f,12] Phenyl rings of adjacent BDC linkers mutually form a weak

(12) (a) Paz, F. A. A.; Klinowski, J. *Chem. Commun.* **2003**, 1484. (b) Rosi, N. L.; Kim, J.; Eddaoudi, M.; Chen, B.; O'Keeffe, M.; Yaghi, O. M. *J. Am. Chem. Soc.* **2005**, *127*, 1504.

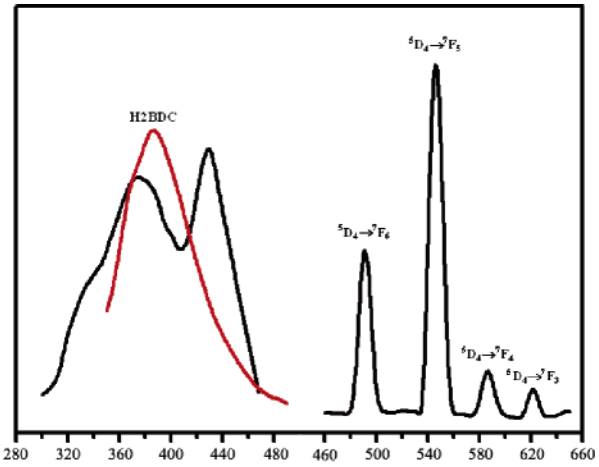

Figure 7. Photoluminescence spectrum of complex **1** excited at 235 nm (black and left) and 254 nm (black and right); Photoluminescence spectrum of free H_2BDC excited at 333 nm (red).

CH···π interaction to lead to an impenetrable organic wall of phenyl groups, which precludes additional ligands from filling between adjacent phenyl groups; thus, an interpenetration structure is prohibited (Figure 4b).[13] Therefore, the coordination modes and the special steric configuration of the BDC linkers result in the discrete inorganic rod-shaped building units and the three-dimensional open framework.

To deeply understand the building units of complex **1**, it is useful to find out how the reported frameworks are constructed from SBUs. Two kinds of SBUs have been well explored by Yaghi's group; they are discrete SBUs and infinite rod-shaped SBUs.[12b] The discrete metal−carboxylate SBUs can be connected by the organic groups as "struts", and the infinite rod-shaped SBUs are joined through organic units as "linkers" to assemble MOFs. The building units of complex **1** have shared the characters of both discrete SBUs and infinite rod-shaped SBUs because the hexameric units are linked to each other through BDC groups as both "struts" and "linkers" (Figure 5). The BDC ligands whose carboxylate groups adopted dimonodentate and chelating/bridging bidentate coordination modes are similar to the "linkers" of the infinite rod-shaped SBUs, and those adopted the chelating bidentate mode like the "struts" to connect the hexameric units.

Thermal Stability and Water Sorption Properties of Complex 1. The thermal stability of complex **1** has been studied using TGA and powder XRD at different temperatures. The TGA, performed from 35 to 800 °C, shows that the first weight loss of 19.48% from 100 to 250 °C corresponds to the loss of all guest molecules (one guest water molecule and one guest DMF molecule) and coordinated solvent molecules (three water molecules and two DMF molecules) (calcd: 19.34%). The decomposition of complex starts above 400 °C, and the remaining weight of 36.88% corresponds to the percentage (calcd: 37.22%) of the Tb and O components, Tb_4O_7 (Figure 6). The powder XRD studies were performed for the as-synthesized sample and the samples heated at 100, 150, and 200 °C, respectively (Figure S2 in the Supportin Information). The powder XRD patterns for samples heated at 100 and 150 °C are similar to that of the as-synthesized sample, which indicated that the departure of the guest molecules does not lead to an obvious phase transformation. When the sample is heated to 200 °C, coordinated solvent molecules begin to depart, which causes a structural transformation with a decrease in crystallinity.

The existence of guest molecules in the microporous frameworks and the thermal stability encourage us to remove the guest molecules and try to create the micropores. The complex **1** is evacuated under reduced pressure (1×10^{-5} Torr) until there is no more weight loss at 150 °C, and then the dehydrated sample is exposed to water vapor sorbate (Figure S1 in the Supporting Information). We observe that about four water molecules per unit cell can be adsorbed into the micropores of dehydrated complex **1**.

Photoluminescent Properties. The photoluminescent spectra of complex **1** and free H_2BDC are shown in Figure 7. Two emission groups for complex **1** in the ranges of 300−480 nm (λ_{ex} = 235 nm) and 460−660 nm (λ_{ex} = 254 nm) are observed. The emission ranging from 460 to 660 nm is attributed to the terbium ion, corresponding to $^5D_4 \rightarrow {}^7F_J$ (J = 3−6).[14] As shown in Figure 6, complex **1** exhibits one blue-shift emission band and one red-shift emission peak with respect to free H_2BDC. The blue-shift emission band at 375 nm would be assigned to the emission of ligand-to-metal charge transfer (LMCT).[15] The red-shift emission peak at 430 nm probably is related to the intraligand fluorescent emission; similar red shifts have been observed before.[16] The emission peak positions of complexes **2**−**4** are similar to those of complex **1**, which would be assigned to the emission of LMCT and the intraligand fluorescent emission according to complex **1**, respectively (Figure S3 in the Supporting Information). These complexes could be anticipated as potential fluorescent materials.

IR Spectrum. The complexes display similar IR spectra. As shown in Figure S4 in the Supporting Information, the asymmetric and symmetric stretching vibrations of the carboxylate groups have bands at 1540 and 1396 cm^{-1}. The bands at 1607, 3066, 851, 680, and 771 cm^{-1} are attributed to the aromatic skeleton vibration of the benzene ring, $\nu_{=C-H}$ of benzene, $\delta_{=C-H}$ out of the face of benzene, and the 1 and 4 substitutions of the benzene ring, respectively. The bands at 1668 and 2929 cm^{-1} are due to $\nu_{C=O}$ and the asymmetric stretching vibration of the methyl group of the DMF molecules. The broad band at 3392 cm^{-1} belongs to the typical band of the water molecules.

Conclusions. Four three-dimensional lanthanide coordination polymers with similar architectures, complexes **1**−**4**,

(13) Rosi, N. L.; Eddaoudi, M.; Kim, J.; O'Keeffe, M.; Yaghi, O. M. *Angew. Chem.* **2002**, *114*, 294.

(14) Zhao, B.; Chen, X. Y.; Cheng, P.; Liao, D. Z.; Yan, S. P.; Jiang, Z. H. *J. Am. Chem. Soc.* **2004**, *126*, 15394.

(15) (a) Dai, J. C.; Wu, X. T.; Fu, Z. Y.; Cui, C. P.; Hu, S. M.; Du, W. X.; Wu, L. M.; Zhang, H. H.; Sun, R. Q. *Inorg. Chem.* **2002**, *41*, 1391. (b) Zhang, L. Y.; Liu, G. F.; Zheng, S. L.; Ye, B. H.; Zhang, X. M.; Chen, X. M. *Eur. J. Inorg. Chem.* **2003**, 2965.

(16) (a) Chen, W.; Wang, J. Y.; Chen, C.; Yue, Q.; Yuan, H. M.; Chen, J. S.; Wang, S. N. *Inorg. Chem.* **2003**, *42*, 944. (b) Thirumurugan, A.; Natarajan, S. *Dalton Trans.* **2004**, 2923.

have been synthesized under mild conditions. XRD analyses reveal that they are crystallized in the triclinic space group $P\bar{1}$. These polymers are constructed from discrete rod-shaped inorganic building units, which link to each other through phenyl groups to lead to three-dimensional open frameworks with rhombic channels along the [0,−1,1] direction. Guest molecules in the framework of complex **1** can be removed to generate permanent microporosity. A water sorption isotherm reveals that four water molecules per formula unit can be adsorbed into these micropores. Because these complexes exhibit strong blue fluorescence and complex **1** shows Tb^{3+} characteristic emission in the range of 450−650 nm, they could be anticipated as potential fluorescent porous materials.

Acknowledgment. This work was funded by the State Basic Research Project (No. G2000077507) and the National Nature Science Foundation of China (Grants 20571030, 20531030, 29873017, 20273026, and 20101004).

Supporting Information Available: CIF files, tables of selected bond lengths and bond angles, chart of coordination modes in complex **1**, and figures of a water sorption isotherm, powder XRD patterns, emission spectra, and an IR spectrum. This material is available free of charge via the Internet at http://pubs.acs.org.

IC0518881